Characteristic curves and the promotion effect of ethanol addition on steam condensation heat transfer

Yoshio Utaka *, Shixue Wang

Division of Systems Research, Faculty of Engineering, Yokohama National University, 79-5 Tokiwadai, Hodogaya, Yokohama 240-8501, Japan

Abstract

Although most previous studies concerning the condensation of binary vapor mixtures report the condensation rates to be less than that for pure vapor, heat transfer enhancement can be realized by using additives to form a positive system (solutal Marangoni condensation). The objective of the present study was to clarify the effect of mixing ethanol into steam on condensation heat transfer. Precise measurements of the ethanol concentration in the vapor of water–ethanol mixtures were performed over a wide range of ethanol concentrations, and the condensation behavior was observed. The maximum heat transfer coefficients in the condensation characteristic curves were determined to be 0.12 and 0.18 MW/m^2 K for vapor velocities of 0.4 and 1.5 m/s, respectively, and appeared at an ethanol vapor mass fraction of approximately 1%. The mixing was demonstrated to be extremely effective, particularly in the low-ethanol concentration range. The condensation heat transfer was enhanced approximately 2–8 times compared to pure steam.
© 2004 Elsevier Ltd. All rights reserved.

1. Introduction

During surface condensation of vapor mixtures of a positive system, where the surface tension of the high-boiling-point component is larger than that of the low-boiling-point component, conditions exist such that, even on wettable heat transfer surfaces, irregular modes of condensate of uneven thickness appear, such as dropwise condensation [1]. The solutal Marangoni condensation phenomena, which is based on the dependency of the surface tension difference between the two liquid components on the concentration of the liquid mixture, is noticeable in vapor mixtures of water and ethanol, for example. An experimental study of gravity-controlled condensation of water and ethanol mixtures on a horizontal tube has been presented by Fujii et al. [2,3]. The group reported five condensation modes: drop, streak, ring, smooth film and wavy film. For vapor

mixtures having ethanol concentrations of 0–20%, the condensate aspect was the same as that for pure water vapor, i.e., film condensation, and the condensation heat transfer coefficient was less than that of pure steam. A later study by Hijikata et al. [4] to examine the condensation characteristics of water–ethanol vapor mixtures on a horizontal plate, in a manner similar to Fujii's group, revealed dropwise condensation for vapor ethanol concentrations of 4–66%, as well as a heat transfer coefficient equal to or less than that of pure steam. Further, Hijikata et al. [5] carried out the theoretical and experimental study concerning the condensation mechanisms of water–ethanol vapor mixture by instability analysis and the heat transfer measurement, in which the values of heat transfer coefficient were relatively low.

On the other hand, an experimental study by Utaka et al. [6,7] using water–ethanol mixtures having vapor ethanol mass fractions of 17–71% revealed that the surface subcooling (cooling intensity) was the essential factor determining the condensate modes and the heat transfer characteristics of solutal Marangoni condensation. Solutal Marangoni dropwise condensation as a

* Corresponding author. Tel.: +81-45-339-3909.
E-mail address: utaka@ynu.ac.jp (Y. Utaka).

pseudo-dropwise mode occurred over a relatively wide range of surface subcooling. The dependence of the heat transfer coefficient on the surface subcooling (condensation characteristic curves) revealed a non-linear nature that was noteworthy, not only due to complex changes in condensation modes, but also to the diffusion resistance inherent as vapor-side thermal resistance in the condensation of the binary mixtures.

In addition, Utaka et al. [6,7] investigated the transition phenomena caused by the changes in condensate modes. With an increase in the subcooling, the condensate modes shifted from smooth film to rivulet, from rivulet to dropwise, from dropwise to dropwise with rivulet, and finally from dropwise with rivulet to smooth film. The condensation heat transfer characteristic curve for the solutal Marangoni condensation exhibits characteristic change with a maximum, as shown in Fig. 1. As mentioned above, the heat transfer characteristics are dependent on the change in condensate modes, which determines the heat transfer resistance of the condensate, and on the diffusion resistance in the vapor phase. Namely, the heat transfer coefficient is very low in the region from point A to point B due to the large diffusion resistance of the vapor phase, even for the dropwise mode of condensate. A decrease in diffusion resistance commences at point B, because the surface temperature of the condensate approaches the boiling point under the vapor–liquid equilibrium relation, as shown in Fig. 2. The steep rectilinear increase to point C in Fig. 1 is a result of the remarkable reduction in diffusion resistance due to the dropwise mode condensate. Hereafter, point B is referred to as the commencement point of the steep increase in heat transfer. The heat transfer coefficient reaches a maximum at heat transfer coefficient point D, then decreases by the transition to film mode at point E.

In the studies described above, the effect of the vapor concentration on solutal Marangoni condensation under the influence of surface subcooling was not considered. Thus, the effect of the vapor concentration has not yet been investigated systematically, and in particular,
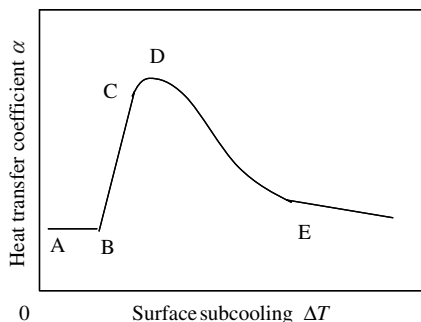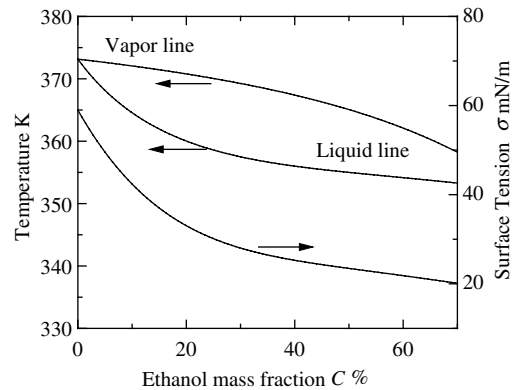

Fig. 2. Phase equilibrium relation and surface tension variation for water–ethanol mixtures.

measurement at low-ethanol concentration has not been reported. The vapor concentration is considered to potentially affect the following: (1) the surface tension of the liquid mixture; (2) the difference in surface tension corresponding to the dew point and the boiling point related to the phase equilibrium, referred to as the overall Marangoni driving force; and (3) the dependence of the diffusion resistance on the concentration of the vapor-side. For low-ethanol concentrations, heat transfer is promoted by an increase in surface tension of the liquid mixture and a decrease in diffusion resistance of the vapor-side due to the decrease in the difference between the compositions of the bulk vapor and the condensate. Conversely, the overall Marangoni driving force is reduced by a decrease in the temperature difference between the dew point and the boiling point. It was thought possible to clarify the quantitative features of solutal Marangoni condensation by measuring characteristic curves over a wide range of vapor concentration.

In this study, the nature of the condensation characteristic curves obtained for water–ethanol mixtures and the influence of the vapor concentration on solutal Marangoni condensation are discussed based on observation of the condensate aspect under multiple vapor velocities and for a wide range of vapor concentrations. In addition, the mechanism for the promotion of heat transfer at low-ethanol concentration is investigated and the promotion effect on steam condensation is discussed.

2. Experimental apparatus and method

A copper heat transfer block, as shown in Fig. 3, devised specifically for investigating phenomena with large heat flux and high-heat transfer coefficients [8] was used. The heat transfer block having a cross-section of

Fig. 1. Condensation characteristic curve for solutal Marangoni condensation.
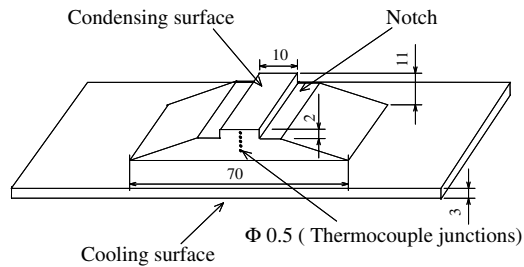
Fig. 3. Condensing heat transfer block.

trapezoidal shape with notches was constructed in order to realize uniformity of surface temperature and large heat flux. The condensing surface had an area of 10 mm × 20 mm.

Oxidized titanium was applied to the condensing surface in order to achieve a wetting surface. In addition, impinging water jets from a bundle of thin tubes were used so as to provide high-cooling intensity uniformly. A schematic diagram of the leak-tight experimental apparatus, intended to minimize the effects of non-condensable gas, is shown in Fig. 4. After passing through the condensing chamber in which the heat transfer block is placed, the vapor generated in the steam generator is condensed almost entirely in the auxiliary condenser. The condensate is returned to the vapor generator by the plunger pump via the flow measurement equipment. The vapor flow is in the same direction in which gravity acts, through a duct of cross-section of 20 × 80 mm. Non-

condensing gas is continuously extracted by the vacuum pump near the outlet of the auxiliary condenser. The inlet of the vacuum pump is cooled by an electronic cooler to maintain a constant concentration in the vapor mixture, by maintaining low-vapor pressure. The loop was divided into a high-pressure part and a low-pressure part bounded by the pressure adjusting valve and the return pump. The vapor pressure of the high-pressure-side is maintained at approximately 1 kPa above atmospheric pressure. The concentration of non-condensing gas in the vapor mixture is measured before and after the experiment. Another heat transfer block for the vapor concentration measurement is attached in the condensing chamber located downstream of the main heat transfer block.

As in previous studies [6,7], after the vapor condition reaches the steady state, the condensation characteristic curves were measured continuously using a quasi-steady measurement in which the temperature of the cooling water was changed very slowly for a fixed concentration and fixed velocity of vapor. The aspect of condensate was observed and recorded through the glass window of the condensing chamber using a CCD camera, and the transition points of the condensate aspect were determined using these photographs.

3. Results and discussion

3.1. Measurement of vapor concentration

We used two methods to determine the ethanol concentration of the vapor mixture. In the first method, the vapor concentration was determined from the vapor–liquid equilibrium relation and measurement of the dew point of the vapor passing through the condensing chamber, as described in previous reports [6,7]. For the dew point measurement in the condensing chamber, precise measurement of the difference in temperature between the heat transfer block and a copper block installed in a container outside the vapor loop, where boiling of pure water occurred, using a thermopile comprised of 10 pairs of thermocouples was performed. In concrete terms, the dew point was determined by measuring the difference between the temperature at the commencement of condensation on the copper block and the boiling temperature of pure water. However, the accuracy of the thermopile (approximately 0.1 K) was insufficient to determine extremely low-ethanol vapor concentrations, due to the small temperature differences.

Therefore, as a second method, the vapor concentration was determined using the vapor–liquid phase equilibrium relation at a given system pressure, as well as the precisely determined concentration of the liquid mixture in the vapor generator for measurements in the
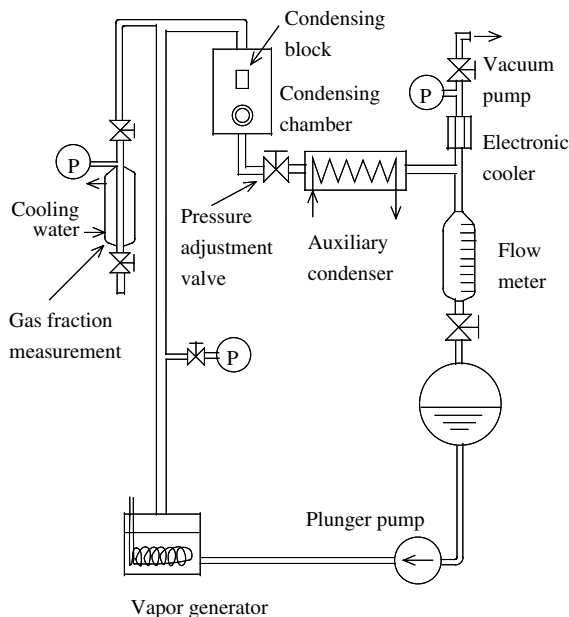

Fig. 4. Schematic diagram of the experimental apparatus.

range of low-ethanol mass fraction below 5%. Based on a study by Utaka et al. [9] on the generated vapor concentration in the boiling process of liquid mixtures, the concentration of bulk generated vapor was found to coincide to that given by the vapor–liquid phase equilibrium relation for the given pressure and liquid concentration, independent of boiling condition. Hence, the vapor concentration in the condensing chamber was dependent on the quantity of condensate in the vapor tube, the stored liquid in the receiver and the concentration difference between vapor and liquid. These values can be considered to be approximately constant for each run. Also, the difference between the vapor concentration in phase equilibrium with bulk liquid and that in the condensing chamber should not be highly dependent on the ethanol concentration. This is because the difference between the concentrations of the dew point line and boiling point line at the same temperature in the range of low ethanol concentration is not so large.

The ethanol mass fractions of the vapor mixtures determined using both measurement methods are shown in Fig. 5 for vapor concentrations at the two vapor velocities. Each point represents the concentration determined using the first method (dew point, plotted along the abscissa) and the second method (liquid concentration, plotted along the ordinate) respectively, for the various mixtures. The values obtained from the two measurement methods coincide fairly well with each other (are within ±10%) in the range of ethanol mass fraction over 5%. Below 5%, the differences between the determined concentrations increase, most likely due to the insufficient precision of the temperature measurements in the first method. The second method was adopted for vapor ethanol mass fractions below 5%. The uncertainty of the vapor mass fraction for the second method seems to be within approximately 10%.
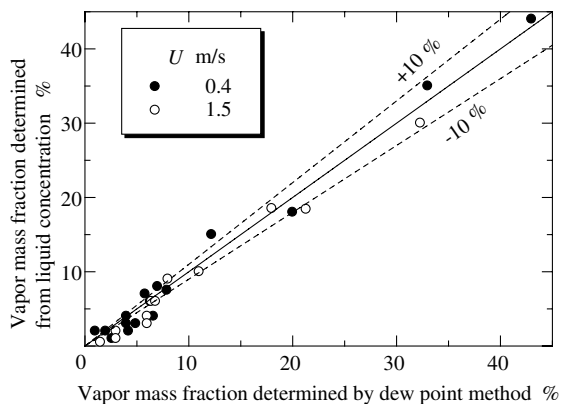
3.2. Condensation characteristic curves

The condensation characteristic curves were measured under fixed vapor pressure and at two vapor velocities (0.4 and 1.5 m/s) for a considerable range of ethanol concentrations. The characteristic curves of the heat flux and the heat transfer coefficient at a vapor velocity of 1.5 m/s are shown for various ethanol concentrations in Fig. 6(a) and (b), respectively. Since film condensation appeared in all subcooling regions for pure water vapor, monotonical change, which is a feature of ordinary film condensation heat transfer, was exhibited for 100% water. In contrast, a common trend was observed for ethanol vapor mass fractions larger than 0.05%. That is, the qualitative features of each curve showed a common characteristic change having heat flux and heat transfer coefficient maxima.

From these characteristic curves, excellent heat transfer characteristics were confirmed, whereby the heat transfer coefficient maxima shifted to the smaller subcooling region and the values at the maxima were very high at low-ethanol concentrations, with the exception of the extremely low-ethanol concentrations of 0.05% and 0.1%. In addition, in the low-ethanol concentration range, the dependencies of the condensation heat transfer characteristics with respect to the

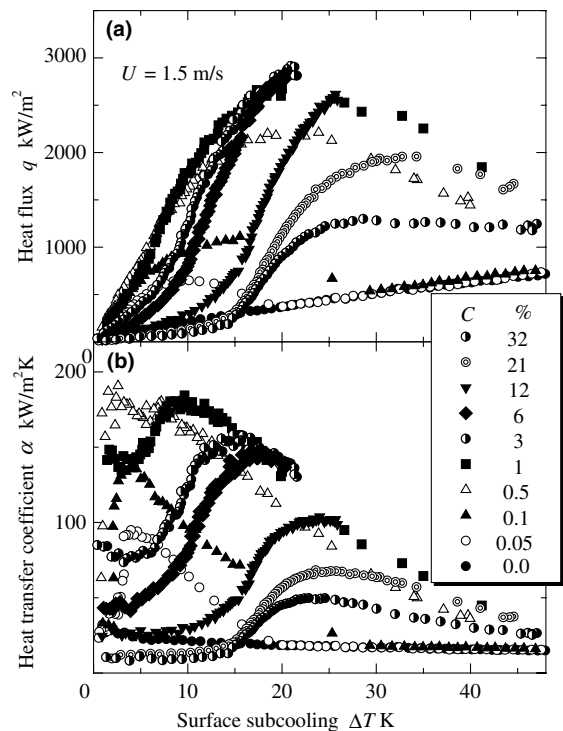Fig. 5. Ethanol mass fraction of the vapor as measured via two methods.

Fig. 6. Condensation heat transfer characteristic curves ($V = 1.5$ m/s).

vapor concentration and the surface subcooling become greater, and the gradient of the characteristic curves at the smaller subcooling range increases. For the vapor velocity of 0.4 m/s (data not shown) the variation in the trend of the curves was similar to that for the vapor velocity of 1.5 m/s.

As indicated in a previous report [6], the realization of excellent heat transfer characteristics is likely due to the following. Since the temperature difference between the boiling point line and dew point line decreases as the ethanol concentration of the vapor mixture decreases, the subcooling region of condensation controlled by the diffusion resistance in the vapor-side becomes narrower. Moreover, since the difference between ethanol concentrations of the vapor in bulk and at the vapor–liquid interface is small and the variation of surface tension with respect to the concentration is large, higher heat transfer conductance is realized. In this study, the concentration of non-condensable gas was 5–12 ppm, and the effects of the non-condensable gas were thought to be very weak [10].

In order to evaluate the condensation characteristic curves quantitatively, we examined the heat transfer quantities at the commencement points of the steep increase in heat transfer, the maximum heat transfer coefficient and maximum heat flux, as well as the condensing surface subcooling. Fig. 7 shows the variation of surface subcooling with respect to vapor ethanol concentration at the commencement points of the steep increase in heat flux and the heat transfer coefficient. From the data, the steep increase in heat transfer is confirmed to have begun approximately when the temperature of the heat transfer surface reached the dew point line temperature. The surface subcooling at the commencement point of the steep increase likely coincided with the temperature difference between the boiling point line and the dew point line in the vapor-phase equilibrium relation. However, the surface subcooling at the steep
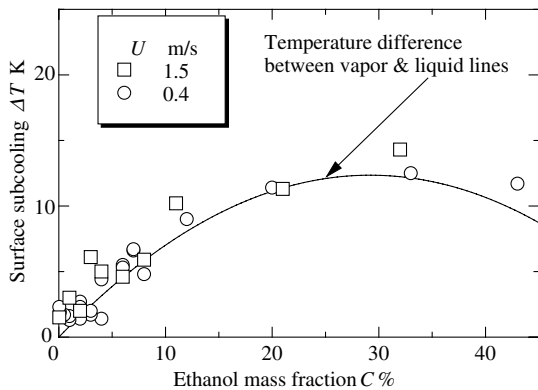
increase point is slightly higher than the temperature difference between the dew point and the bubble point in the vapor–liquid phase equilibrium, and is almost constant in the low-concentration range of less than 3% ethanol.

Fig. 8(a) and (b) show the changes in the maximum heat flux and heat transfer coefficient, respectively, with the condensing surface subcooling, the maximum values of which appear in the region of low ethanol concentration. When the vapor velocity was 0.4 m/s, a maximum heat flux of approximately 1.7 MW/m^2 appeared at an ethanol concentration of approximately $C = 6\%$. The surface subcooling at the maximum value of heat flux increased monotonically with respect to the vapor concentration, and the rate of increase was relatively high in the low-concentration range. When the vapor velocity was 1.5 m/s, a maximum heat flux could not be directly obtained due to insufficient cooling intensity and excessive heat flux. Assuming a similar trend in behavior as for the vapor velocity of 0.4 m/s, the maximum heat flux at vapor velocity of 1.5 m/s was estimated to be
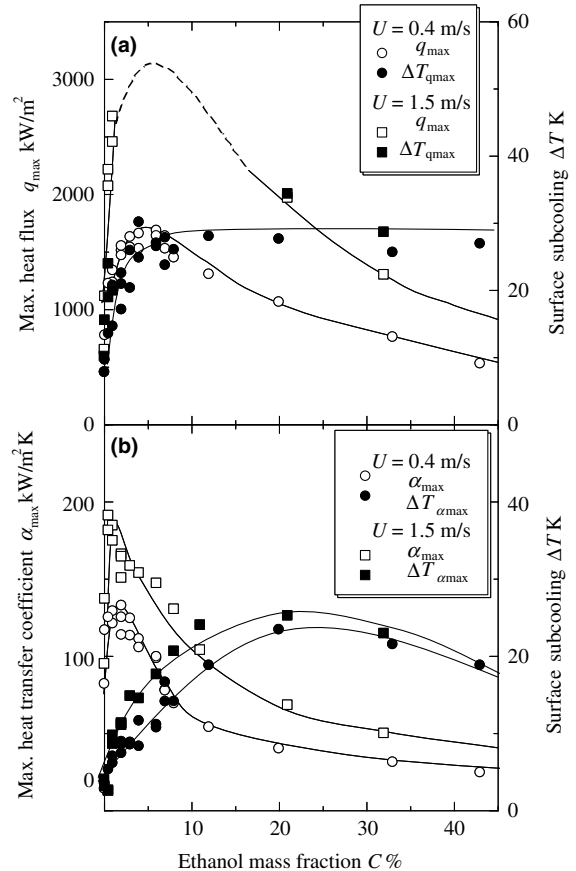

Fig. 7. Surface subcooling at the steep increase point of heat transfer.

Fig. 8. Characteristics of maximum values of heat transfer. (a) Maximum heat flux (b) Maximum heat transfer coefficient.

approximately 3 MW/m², as indicated by the dotted line in Fig. 8(a). As shown in Fig. 8(b), the maximum heat transfer coefficients appeared at an ethanol concentration of approximately $C = 1\%$, and were 0.12 and 0.18 MW/m² K for vapor velocities of 0.4 and 1.5 m/s, respectively. In addition, the subcooling at the maximum heat transfer coefficient showed some variation, with a peak that appeared at a vapor concentration of approximately 20%.

3.3. Transition of condensation modes

In this study, for all water–ethanol vapor mixtures examined, the aspects of condensate were observed to shift from smooth film to rivulet, from rivulet to dropwise, from dropwise to dropwise with rivulet, and finally from dropwise with rivulet to smooth film, with the increase in the surface subcooling. Fig. 9 shows the range of typical condensation modes as determined from observation using the CCD camera. The transition points of the condensation modes from film to rivulet, from rivulet to dropwise, and from dropwise with rivulet to film are denoted by the symbols ○, △, and □, respectively. The hatched area between the two solid lines shown in the figure denotes the range of dropwise mode. The subcooling range over which the irregular condensate aspect occurred exists for all concentrations of vapor mixtures, and the subcooling at the transition point from film to rivulet was less than 2 K approximately, indicating that irregular condensation can be realized over a wide range of vapor concentrations and surface subcooling. In addition, the boundary between the rivulet mode and the dropwise mode was approxi-
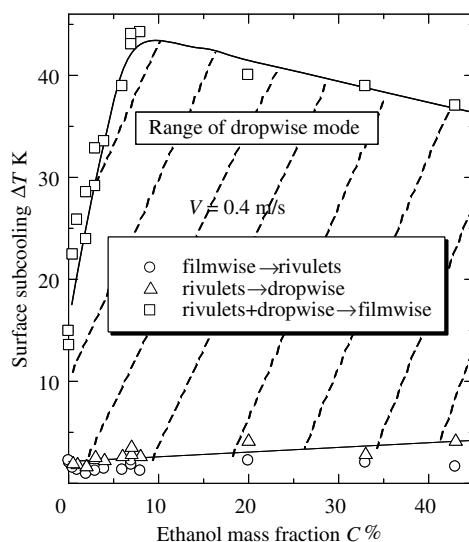
mately 2–3 K in the low-ethanol-concentration range, as indicated by the straight line determined by the least squares method. The subcooling at the transition points exhibited an increasing trend along with increasing ethanol concentration. The reason for this is that the gradient of the surface tension versus the condensate mass fraction becomes larger with the decrease in vapor concentration.

From Figs. 7 and 9, in the ethanol vapor concentration region of less than 3% the surface subcooling at the commencement points of the steep increase in heat transfer is approximately equal to that of the transition points of the condensate aspect change from film to rivulet or dropwise mode. In the vapor concentration region over 3%, the surface subcooling at the commencement points is greater than the surface subcooling at the transition points of the condensate aspect change to the rivulet or dropwise mode. This indicates that the control mechanism of the condensation heat transfer for the subcooling region changes at a vapor ethanol concentration of approximately 3%. In other words, in the vapor concentration region of less than 3%, the mechanism is controlled primarily by the thermal resistance of the condensate, while in the vapor concentration region over 3%, the controlling mechanism changes primarily to vapor-side diffusion resistance.

3.4. Theoretical analysis of diffusion resistance and the nature of the condensation curves

For solutal Marangoni condensation, the condensate resistance based on the condensate aspect and the mass diffusion resistance in the vapor-side is fundamental in controlling the condensation characteristics. This phenomenon consists of the unsteady process whereby the condensate thickness and the vapor concentration change due to the variation of the condensate mode. An analysis of the diffusion resistance of the vapor-side is required in order to explain the detailed mechanism. The relation between the condensate aspect and the condensation characteristic was previously reported by one of the present authors [11].

Here, a model approximating the process just after sweeping by a departing drop in a typical condensation process was considered along with the diffusion resistance. Rapid condensation occurs with the beginning of sweeping of the heat transfer surface by a departing drop. The concentration distribution proceeds due to rapid condensation from the initial situation where the heat transfer surface is covered by a large drop with comparatively lower heat transfer and uniform concentration distribution. By solving a one-dimensional unsteady diffusion equation derived from the idealized process described above using a numerical method, the thermal conductance variation of the vapor-side for a process in which the condensation occurs swiftly from

Fig. 9. Variation of the range of irregular condensate with respect to ethanol mass fraction and surface subcooling.

uniform concentration is investigated. In particular, the variations of the characteristic points of the condensation characteristic curves, as shown in Fig. 8(a) and (b), were investigated.

The vapor–liquid interface temperature is given as a boundary condition in order to consider only the conductance in the vapor phase. In addition, since Utaka and Nishikawa [12] reported that the condensate film thickness was very thin, approximately 1 μm, in the surface subcooling range near the maximum heat transfer coefficient, the thermal resistance of the condensate film is small and the surface temperature of the condensate liquid is near that of the heat transfer surface. The basic equation, the boundary conditions, and the initial condition can be written as

$$\frac{\partial C}{\partial t} + V\frac{\partial C}{\partial y} = D\frac{\partial^2 C}{\partial y^2} \tag{1}$$

$$y = 0 : C = C_I \tag{2}$$

$$\left(\rho D\frac{\partial C}{\partial y}\right)_I = (C_{IL} - C_I)m \tag{3}$$

$$m = \rho V \tag{4}$$

$$y = \infty : C = C_\infty \tag{5}$$

$$t = 0 : C = C_\infty \tag{6}$$

where C is the ethanol mass fraction of the water–ethanol vapor mixture, D is the diffusivity between water and ethanol, V is the velocity of the vapor flowing into the heat transfer surface due to the condensation, ρ is the vapor density, m is the condensation rate, and C_I, C_{IL} and C_∞ are the ethanol concentrations of vapor and liquid in the vapor–liquid interface and the vapor concentration in bulk, respectively. The thermal conductance H and the non-dimensional temperature difference ΔT^* in the vapor phase are defined respectively as

$$H = Lm/(T_S - T_I) \tag{7}$$

$$\Delta T^* = (T_S - T_I)/(T_S - T_L) \tag{8}$$

where L is the latent heat of condensation, T_S and T_L are the dew point and boiling point, respectively, corresponding to the vapor concentration C_∞ in the phase equilibrium diagram of water and ethanol, and T_I is the temperature of the vapor–liquid interface.

Fig. 10 shows the time variation of the concentration distribution in the vapor phase. It is seen that the thickness of different concentration region becomes thicker with time. Fig. 11 shows the variation of thermal conductance against the non-dimensional temperature difference in the vapor phase for the different bulk vapor concentrations, calculated when the time equals 0.1 s. Assuming a similar distribution of the condensate shape, the period of frequency between drop departures is in-
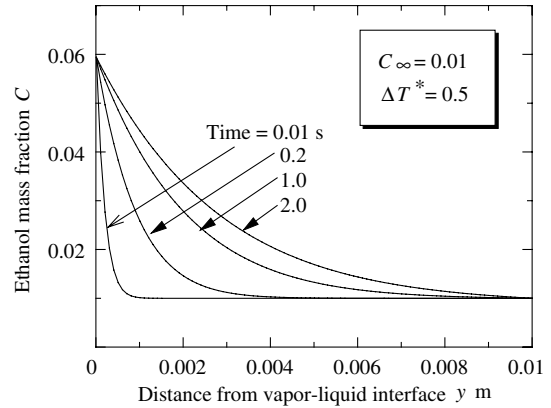

Fig. 10. Variation of distribution of mixture vapor concentration with time.
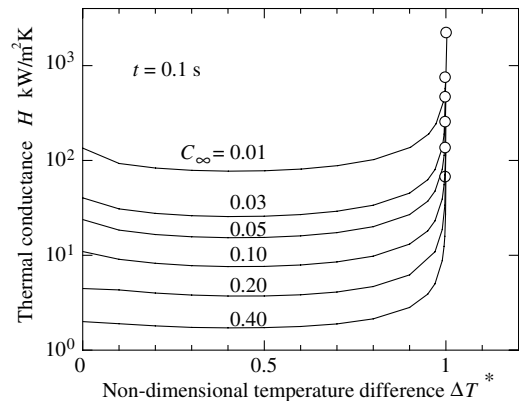

Fig. 11. Variation of thermal conductance with respect to non-dimensional temperature difference in the vapor layer ($t = 0.1$ s).

versely proportional to the heat flux. Therefore the characteristic time is dependent on that period. Also, the maximum heat flux of such a diffusion process is different for different vapor concentrations. However, for convenience, the thermal conductance at a fixed time is compared in order to examine the character of the variation in the condensation characteristic curve and its characteristic points. Since the sweeping period by the departing drop is approximately 0.1–0.2 s at the maximum heat transfer coefficient on the condensation characteristic curves, the calculation result for this time was adopted herein.

As a characteristic of the vapor-side diffusion resistance, the heat flux tends to increase rapidly for any vapor concentration when the non-dimensional temperature difference approaches 1.0 (i.e. the vapor–liquid interface temperature approaches the boiling point),

because the compositions of the condensation and the bulk vapors also approach each other. Thus, it is understood that subcooling at the commencement point of the steep increase in heat transfer coincided with the temperature difference between the dew point and boiling point, as shown in Fig. 7. Moreover, the decrease in the diffusion resistance in the vapor-side due to the decrease in ethanol concentration improved the heat transfer performance. This is thought to be one of the reasons why a relatively high-maximum heat transfer coefficient appears in the low-vapor-concentration region.

Next, the influence of vapor concentration on the condensate side was examined. As shown in Fig. 2, the gradient of the surface tension with respect to the concentration increases with a decrease in ethanol concentration of the vapor mixture. Thus, the driving force becomes stronger and the condensate resistance becomes weaker, which causes the condensate to become irregular. However, when the ethanol concentration decreases significantly, the temperature difference between dew point and boiling point in the vapor–liquid phase equilibrium diagram becomes very small. Therefore, the surface tension difference that can be formed on the condensate surface will decrease regardless of the surface tension gradient. In the very-low-vapor-concentration range, the heat transfer coefficient will decrease with a decrease in ethanol concentration because the overall driving force of irregular condensation becomes weak and the condensate resistance increases. Thus, the heat flux and the heat transfer coefficient show a maximum with respect to the vapor concentration due to (1) the increase in the surface tension gradient with respect to the concentration of the liquid mixture and the decrease in the diffusion resistance in the vapor-side with a decrease in ethanol concentration of the vapor mixture, and (2) the decrease in the surface tension difference, which is determined by the dew point and the boiling point as the overall Marangoni driving force in the very-low-ethanol-concentration region.

3.5. Promotion of steam condensation by addition of ethanol

In this last section, we examine the promotion of condensation heat transfer by adding ethanol to water. Fig. 12 shows the variation of the condensation heat transfer coefficient of the vapor mixture normalized by that of pure steam with respect to the subcooling, for a vapor velocity of 0.4 m/s. For all vapor concentrations, the maximum shifted slightly from that of the characteristic curve toward larger subcooling. This is due to the lowering of the heat transfer coefficient for pure steam with the increase in subcooling. The condensation heat transfer was improved over almost the entire measured subcooling region for ethanol concentrations of less
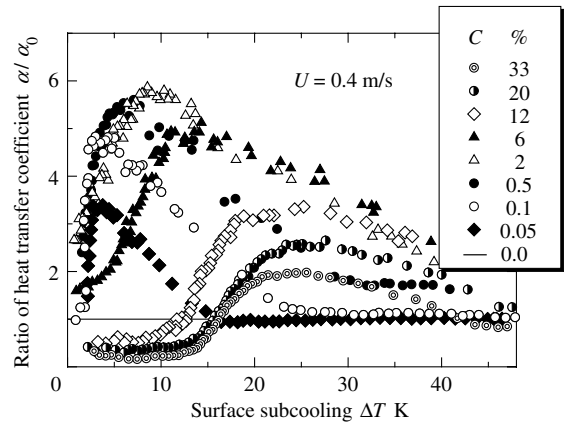

Fig. 12. Ratio of the condensation heat transfer coefficient of the mixture vapors to that of pure steam, with respect to surface subcooling.

than approximately 6%. On the other hand, when the ethanol concentration of the vapor mixture was higher than 12%, the ratio of condensation heat transfer of the vapor mixture is smaller than that of steam in the low-subcooling region, but is higher in the subcooling region larger than that of the commencement point of steep increase. As discussed in Section 3.4, the mutual relationship of the Marangoni driving force on the condensate and the diffusion resistance in the vapor phase in the condensation of binary vapor mixtures determines the condensation characteristics. The decrease in condensation heat transfer coefficient due to the diffusion resistance of the vapor-side is relatively small in the case of $C \leqq 6\%$ for low-ethanol concentration. In the case of $C \geqq 12\%$, as the diffusion resistance is the controlling factor, the condensation heat transfer coefficient was reduced even in the dropwise mode.

Fig. 13 shows the relationships between the ethanol concentration of the vapor mixture and the maximum value of the ratio of the heat transfer coefficient of the vapor mixture, α, to steam, α_0, with respect to the surface subcooling. For an ethanol concentration of approximately 1%, the addition of ethanol improves the condensation heat transfer coefficient of the mixture, compared to steam, by a factor of approximately six at a vapor velocity of 0.4 m/s, and by a factor of approximately eight at a vapor velocity of 1.5 m/s. In addition, for vapor concentrations of 0.05% and 0.1% (ethanol concentrations of the liquid mixture were 0.005% and 0.01%, respectively), which are very low, the ratios of the heat transfer coefficients reached 3.5–5.5, and the subcooling is in the relatively small temperature difference range of approximately 3–5 K. Thus, the addition of a very small amount of ethanol is expected to promote the heat transfer process for a comparatively small temperature difference and at sustained high-heat transfer
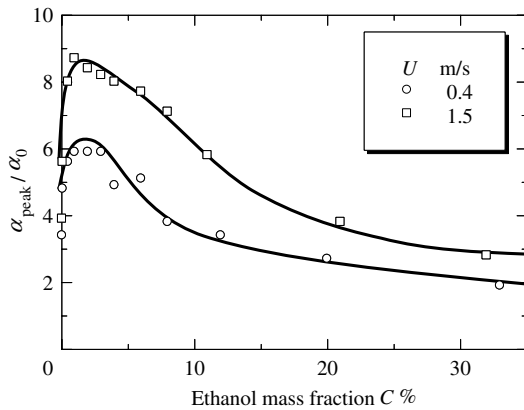
Fig. 13. Variation of the peak ratio of the condensation heat transfer coefficient of the mixture vapors to that of pure steam, with respect to the ethanol concentration in the mixture vapors.

coefficient regardless of the nature of the condensation surface.

4. Conclusions

The promotion of steam condensation heat transfer via solutal Marangoni condensation phenomena was investigated using a leak–tight apparatus to minimize the effects of non-condensing gas. The obtained results are summarized as follows:

1. In order to clarify the effect of vapor concentration on the condensation heat transfer characteristics for water–ethanol solutal Marangoni condensation, condensation heat transfer characteristic curves were measured for a wide range of vapor concentrations at vapor velocities of 0.4 and 1.5 m/s. The characteristic curves for heat flux and the heat transfer coefficient exhibited non-linear change and had maxima with respect to the surface subcooling for all vapor concentrations and both velocities. Moreover, the maxima of heat flux and the heat transfer coefficient appear at ethanol concentrations of approximately 6% and 1%, respectively. The maximum heat transfer coefficient reached 0.12 and 0.18 MW/m^2 K for vapor velocities of 0.4 and 1.5 m/s, respectively.
2. Observation of the condensate aspect and the commencement point of the steep increase in heat transfer revealed that the control mechanism of solutal Marangoni condensation heat transfer in the low subcooling region changed at a vapor ethanol concentration of approximately 3%.
3. By comparing the condensation heat transfer coefficients of the vapor mixtures and pure steam, the promotion effect on steam condensation heat transfer by the addition of ethanol was investigated. The promotion effect of adding an extremely small amount of ethanol was remarkable, reaching a factor of approximately 8 at the highest.
4. The mechanism for the promotion of heat transfer was investigated by using diffusion analysis and the condensate behavior. It was suggested that the factors involved in the promotion due to vapor concentration are (1) the increase in the surface tension gradient with respect to the concentration of the liquid mixture and the decrease in the diffusion resistance in the vapor-side with a decrease in ethanol concentration of the vapor mixture, and (2) the decrease in the surface tension difference.

References

[1] V.V. Mirkovich, R.W. Missen, Non-filmwise condensation of binary vapor of miscible liquids, Can. J. Chem. Eng. 39 (1961) 86–87.
[2] T. Fujii, S. Koyama, Y. Shimizu, M. Watabe, Y. Nakamura, Gravity controlled condensation of an ethanol and water mixture on a horizontal tube, Trans. Jpn. Soc. Mech. Eng. (Series B) 55 (509) (1989) 210–215.
[3] T. Fujii, N. Osa, S. Koyama, Free convection condensation of binary vapor mixtures on a smooth horizontal tube: condensing mode and heat transfer coefficient of condensate, Proc. US Eng. Found. Conf. (1993) 171–182.
[4] Hijikata K, Nakabeppu O, Fukasaku Y, Condensation characteristics of a water–ethanol binary vapor mixture. In: Proc of 29th Japan Heat Transfer Symp, 1992, p. 742–3.
[5] K. Hijikata, Y. Fukasaku, O. Nakabeppu, Theoretical and experimental studies on the pseudo-dropwise condensation of a binary vapor mixture, J. Heat Transfer 118 (1996) 140–147.
[6] Y. Utaka, N. Terachi, Measurement of condensation characteristic curves for binary mixture of steam and ethanol vapor, Heat Transfer Jpn. Res. 24 (1) (1996) 57–67.
[7] Y. Utaka, N. Terachi, Study on condensation heat transfer for steam–ethanol vapor mixture (Relation between condensation characteristic curve and modes of condensate), Trans. Jpn. Soc. Mech. Eng. (Series B) 61 (588) (1995) 3059–3065.
[8] Y. Utaka, S.X. Wang, H. Kobayashi, Determination of configuration of heat transfer block to realize large heat

flux and high precision of measurement for high thermal conductance phenomena, Trans. Jpn. Soc. Mech. Eng. (Series B) 67 (660) (2001) 2041–2047.

[9] Y. Utaka, T. Takahashi, T. Tsuboi, Study of vapor concentration during boiling process of binary liquid mixtures, Heat Transfer—Asian Res. 31 (8) (2002) 595–605.

[10] S.X. Wang, Y. Utaka, Effect of non-condensable gas on solutal Marangoni condensation heat transfer characteristics for water–ethanol vapor mixture, Trans. Jpn. Soc. Refrigerat. Air Condition. Eng. 19 (4) (2002) 313–320.

[11] Utaka Y, Kenmotsu T, Yokoyama S, A study on Marangoni condensation (measurement and observation for water and ethanol vapor mixture). In: Proc 11th Int Heat Transfer Conf, vol. 6, 1998, p. 397–402.

[12] Y. Utaka, T. Nishikawa, Measurement of condensate film thickness for solutal Marangoni condensation applying laser extinction method, J. Enhanc. Heat Transfer 10 (1) (2003) 119–129.